

Strength Optimization and Strength Prediction of Fused Deposition Modelled Specimens Based on Process Parameters

Maurice P. Schwicker¹, Nikolay D. Nikolov², and Marco Hässel¹

¹University of Applied Sciences – Kaiserslautern, Department of Applied Engineering Sciences, Kaiserslautern, Germany

²Technical University of Sofia, Department of Mechanics, Sofia, Bulgaria

Email: Maurice.Schwicker@hs-kl.de, Marco.Haessel@hs-kl.de, nyky@tu-sofia.bg

Abstract—There are many factors, which influence the strength of parts produced by Fused Deposition Modeling. In this study, the effects of main manufacturing process parameters are quantified and optimized using the Design of Experiment approach, in order to produce components with higher tensile strength. First, the main manufacturing parameters, which can be set in the slicing software, are explained. Ten parameters are selected for strength optimization, using standard tensile test specimens. The strength and elasticity modulus resulting from the parameters sets are determined and evaluated. It was found that the nozzle diameter, top and bottom layer orientation, infill amount and layer height have a major influence on strength. Additionally, the effects of filament color and time after building are examined and their effect on strength was found to be negligible. A regression model is developed to calculate optimized parameter sets. The model was verified, resulting in a 7% higher tensile strength than the strongest specimen in the experiment design. Using the same model, an equation for prediction of tensile strength is proposed.

Index Terms—fused deposition modelling, strength optimization, strength prediction, design of experiment, process parameters

I. INTRODUCTION

Over the past few years, the Fused Deposition Modelling (FDM) process has undergone significant development in the fields of optimization, application, and software support. Through series production, 3D printers are not only found in industry, but also in private households. More and more processes are being developed that accelerate Additive Manufacturing (AM) processes and improve the quality of components [1]-[4]. AM has great potential in many areas as parts can be constructed with a focus on function and less on manufacturability due to the increased design freedom. Various parameters influence the mechanical strength and surface quality [5]-[7]. For example, a larger nozzle diameter decreases surface finish, but increases printing speed [8]. Increasing the layer height while keeping the nozzle diameter constant, creates air gaps in the part [9]. Change in

temperature can drastically affect the bonds of the extruded strands. Hence, AM plastic components have a lower strength than injection-molded ones, so that the strength is not only limited by the material but also by the process. In this work, the relevant manufacturing parameters are determined and optimized, in order to achieve maximum tensile strength using the FDM process. The material used is polylactide, being one of the most widely used plastics in the filament market. In order to collect the data as systematically and model-oriented as possible, the Design of Experiment (DoE) approach was chosen. Separately investigated parameters will be used to further validate results.

II. TEST EQUIPMENT AND APPROACH

The specimens were built with a Renkforce RF2000 3D printer, using the system shown in Fig. 1(a). The tensile tests are carried out on a Zwick 1475 universal testing machine, Fig. 1(b). The specimens built have a standard ISO 527-1A shape and sizes [10], shown in Fig. 1(c).

The tension tests were conducted with a preload of 0.1 MPa. The modulus of elasticity E was measured with a test speed of 1 mm/min. If the linear-elastic range is exceeded, the test speed increases to 20 mm/min and the specimen is pulled to fracture. The test temperature for all tests is room temperature. To avoid damaging the specimens during clamping in the testing machine or pulling them out of the clamping jaws during the tensile test, own measurements were made. They have shown that the clamping pressure of 2 MPa is sufficient for all samples and that the distance between the clamping jaws must be varied between 3.7 mm and 3.9 mm depending on the sample.

The software Simplify3D® was used as slicer and Minitab® as a statistical software to develop and evaluate the DoE. Specimens which fractured at the clamping area were omitted from the analysis.

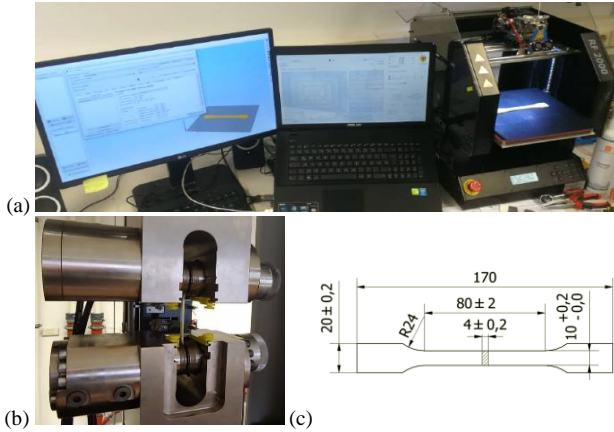


Figure 1. Equipment used: (a) Renkforce RF 2000 with PC and Simplify3D® slicer software; (b) Zwick type 1475 tensile testing machine (clamps shown) (c) Dimensions of ISO527-1A specimen.

III. INVESTIGATED PARAMETERS

Within the Simplify3D® slicer software about 100 parameters can be set, some of which have a greater influence on the strength than others. The most important manufacturing parameters are presented as a first step.

In order to effectively perform a parameter study, the number of samples to be printed and the number of measurements to be performed shall be as small as possible and at the same time as high as necessary. The most relevant parameters for strength and surface quality are then included in the respective experimental design, summarized in Table I and illustrated in Fig. 2.

A. Nozzle Diameter

The plastic is extruded through nozzles with available diameters of 0.3 mm, 0.4 mm and 0.5 mm. The smallest and largest possible nozzle is used for the test plan.

B. Extrusion Width

This parameter describes the width of the strands to be extruded as well as the center to center distance of the strands – Fig. 2(a). As this width is mainly dependent on the nozzle diameter, a factor 0.9 and 1.1 times the nozzle diameter is used in the DoE. The values were chosen to reveal the influence of values smaller and larger than the nozzle diameter.

TABLE I. PARAMETERS CONSIDERED IN THE PARAMETRIC STUDY

No.	Parameter	Symbol	Lower value (L)	Higher value (H)
1	Nozzle diameter	d_N	0.3 mm	0.5 mm
2	Extrusion width-multiplier	W_E	$0.9 \times d_N$	$1.1 \times d_N$
3	Layer height	h_l	0.1 mm	0.3 mm
4	Infill density	I	50%	90%
5	Outline overlap	O_O	15%	35%
6	Print Speed	v	1000 mm/min	3000 mm/min
7	Extrusion temperature	T_E	200 °C	220 °C
8	Print-bed temperature	T_B	70 °C	90 °C
9	Top & bottom layer orientation	O_P	0 °	90 °
10	Infill pattern	$P\#$	1 – Rectangular 2 – Grid 3 – Triangular 4 – Full Honeycomb	

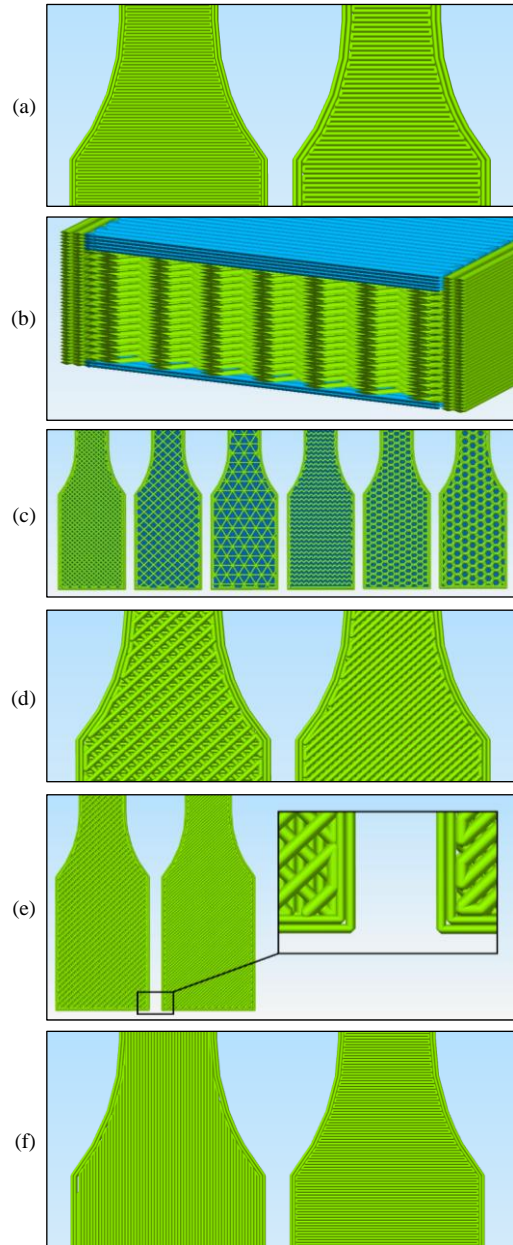


Figure 2. Parameters influencing strength: (a) Nozzle diameter and Extrusion width; (b) Top, bottom, and side layers; (c) Infill patterns – rectilinear, grid, triangular, wiggly, fast honeycomb, and full honeycomb; (d) Infill density; (e) Outline overlap – left 15%, right 0%; (f) Top and bottom layer orientation – 0° and 90°.

C. Primary Layer Height

This parameter is used to set the thickness of a layer. It is an important influencing factor on the strength and the surface quality, so that it is considered in the experimental design on the steps 0.1 mm and 0.3 mm. There are also special settings for the first layer on the printing bed. These include the “first layer height”, the “first layer width” and the “first layer speed”. These settings can help prevent the component from being detached during printing. As these parameters are primarily responsible for stabilizing the process and ensuring print-bed adhesion, they are ultimately not relevant for strength and surface optimization. Different types of layers are illustrated in Fig. 2(b).

D. Infill Pattern

The infill is located between the upper and lower solid layers and can be adjusted. Some of the possible patterns are shown in Fig. 2(c). From left to right: “rectilinear”, “grid”, “triangular”, “wiggle”, “fast honeycomb” and “full honeycomb”. For the experimental design, the infill pattern “wiggle” is neglected, as it will have worse strength properties than the other patterns due to the non-contiguous geometry. Furthermore, for the experimental design only one of the two honeycomb patterns, the full honeycomb pattern, is considered. To account for the four different infill patterns in a $2k$ -partial factorial experimental design, they are realized as 4 blocks. The influence of the infill pattern is thus considered but cannot be evaluated together with the main effects. In order to evaluate the infill pattern quantitatively, four additional experiments are inserted, in which only the infill pattern is varied, and the remaining factors are kept constant.

E. Infill Density

The amount of infill is controlled by the “infill percentage”, Fig. 2(d), from 0 % to 100 %. Since a higher infill leads to a higher strength as the area of the cross-section increases. The steps for the design in the upper percentage range are set at 50 % and 90 %. An infill of 100 % is not sensible if the effects of the infill pattern have to be examined. Although it is already known that a higher infill leads to an increase in strength [5], this investigation quantifies the effect of its change in connection to the other parameters.

F. Outline Overlap Percentage

This parameter, shown in Fig. 2(e), defines the percentage of the extrusion width, which overlap between the infill strands and the outline shells and ensures bonding. Since the value defined in the standard settings is 15 %, the steps 15 % and 35 % are examined for strength optimization.

G. Print Speeds

The print speed sets the velocity of the nozzle when printing, thus affecting the linear drives of the X and Y axes and the extruder motor. Speeds are included in the study since the melt flow speeds change at different extruder temperatures and may cause interactions with the printing speed. If the extruder temperature is 190 °C, the melt flow rate is 0.30 g/min and if the extruder temperature is 210 °C, the melt flow rate is 0.81 g/min according to the filament manufacturer Verbatim™. Also, higher speeds result in increased vibration of the machine, which may affect bonding strength of the layers. The preset from the slicing software for the “global print speed” is 3000 mm/min. Therefore, strength optimization levels of 1000 mm/min and 3000 mm/min are selected, speculating that a slower speed might increase bonding between the layers. The contour and infill speed, which control the traversing speed when printing the outline shells or infill, can be adjusted separately which is not investigated in the current study. For the print speed of the shells, the levels 40 % and 100 % of the global print speed are used.

H. Extrusion Temperature

The used filament diameter is 2.85 mm. The filament manufacturer (Verbatim™) specifies an extrusion temperature of 200 °C to 220 °C. Accordingly, the temperature steps 200 °C and 220 °C are selected. As a rule of thumb, a higher temperature discourages clogging the extruder and encourages better bonding of the strands.

I. Print-bed Temperature

The filament manufacturer recommends print-bed temperature of 80 °C in the data sheet. Accordingly, the temperature steps 70 °C and 90 °C for the print-bed are selected. Since the glass transition temperature of PLA is 60 °, a higher temperature of the print-bed may encourage bonding of the lower layers.

J. Top and Bottom Layer Orientation

The orientation of the bottom and top layers plays a significant role, as its change results in different interfaces of the strands being stressed. For example, specimens printed with strands perpendicular to the load direction are primarily stressed at the interface between the strands, not the cross-sectional area of the strands. This results in anisotropic behavior. The experimental design uses an orientation of 0 ° and 90 °. These orientations are shown in Fig. 2(f).

All considered parameters with their designations and respective steps are shown in Table I.

K. Separately Investigated Parameters

In order to measure the influence of time on tensile strength, specimens with the identical process parameters were printed and divided into two groups. One group was tested one day after the print, the second group – thirty days after the print date. Additionally, two prints with identical process parameters, but with different filament colors were produced to detect whether the color pigments have any influence on strength.

L. Parameters Not Included in the Study

“Extrusion multiplier” or “flow rate” is an important parameter regulating the extruded length of filament per time unit. It is often used to calibrate dimensional accuracy and adjusted during printer calibration to obtain the correct flow rate of filament, depending on the specific machine used.

Standing specimens and specimens demanding support structures are not included in the DoE. Therefore, the effect of loads stressing the layer-layer interface were not investigated. Also, the effect of notches at the specimen surface due to support structures is not included.

There are additional options for setting up “top solid layers”, “bottom solid layers” and “outline shells”. Depending on the size of the part, the surface ratio of solid layers to infill layers in a cross-section is different, even if the associated parameters remain constant. So, a variation of these parameters in the test plan for strength optimization is not sensible if the ISO 527-1A standard is used. Hence, the Simplify3D® default settings – three bottom, three top layers as well as two outline shells were set for the whole DoE.

There are additional parameters, which prevent stringing, unwanted gaps between layers and splitting. These settings include the “retraction distance”, which is the distance that the filament is retracted back into the nozzle when it is not extruding. The “extra restart distance” indicates the added distance of the filament in the nozzle to compensate for lost melt during a travel move. This value can especially affect standing specimens which have much more layers. Little over- or under extrusions may occur at every retraction, altering the cross-section of the part. “Retraction vertical lift” defines the distance that the nozzle removes from the print object when changing the print position in the direction of the z-axis.

There are also many other aids like brims, prime pillars, and ooze shields. However, these are additional parameters stabilizing the printing process. Once optimized for the printer, they do not affect the quality of the specimens and are therefore not included in the DoE.

IV. EXPERIMENTAL DESIGN

For a full factorial design plan with two steps, excluding the four infill patterns, the number of experiments would amount to $n = n_i^{k-p} = 2^{(10-1)-0} = 512$ experiments, with n being the required number of experiments, n_i – the number of levels per factor, k – the number of factors and p – the reduction level. To ensure repeatability each specimen in the DoE needs to be printed three times. This is not efficient for reasons of time and cost, so a partial factorial experimental design plan was used. The purpose of a partial factorial experimental designs is to get by with as few experiments as possible while minimizing the loss of information. Each experimental design represents a linear system of equations. Thus, in the case of a full factorial design with four factors and two levels each, a description model with 16 constants can be set up. Four constants are allotted to the main effects, six constants to the twofold interactions, four to the threefold interactions, one to the fourfold interaction and the last one to the total mean. The

strategy of the partial factorial experimental designs now starts from the approach that the model constants of higher order do not reach significant values and are ultimately not relevant. The overall mean and main effects can be determined with confidence using the partial factorial experimental design, but there remains uncertainty for the two-way interactions. This is the price that was accepted for increased efficiency.

The resolution of an experimental design is measured by the order of effects that are confounded. When running a partial factorial design, certain effects are intermingled, so they cannot be estimated separately. Usually, the use of a partial factorial experimental design is aimed at the highest possible resolution for the required fractionation. Hence, a partial factorial experimental design plan with a resolution of IV using 9 factors was created with two levels, reducing the experiments from 512 to $n_r = n_i^{k-p} = 2^{(10-1)-3} = 64$ experiments.

In order to keep the measurement error as low as possible and to ensure successful statistical evaluation, three samples were printed for each test, including the additional investigations to check reproducibility.

The four different infill patterns in a partial factorial experimental design are realized as four blocks. The influence of the infill pattern is thus considered but cannot be evaluated in effect plots. To assess the infill pattern quantitatively, four additional experiments ($n_p = 4$) were added, in which only the four infill patterns are varied, and the remaining 9 factors are kept constant. The value of these factors was set as mean values of the level corners and marked as “0” in Table II.

For example, the nozzle diameter steps were set to 0.3 mm and 0.5 mm. Hence, the nozzle diameter of 0.4 mm was used for investigating the infill patterns. This allowed to treat these investigations as center point measurements and benefit validity. These center point measurements were repeated six times. This results in a total of 68 experiments. Thus, the total amount of necessary specimens is $n_s = 3n_r + 6n_p = 3 \times 64 + 6 \times 4 = 216$.

TABLE II. DOE PLAN

№	31	6	14	17	41	46	57	58	67	3	8	11	20	30	40	42	64	32	4	13	21	44	48	53	62	66	1	5	12	26	33	49	50	56
d_N	0	H	H	H	H	H	H	H	H	L	L	L	L	L	L	L	L	0	H	H	H	H	H	H	H	H	L	L	L	L	L	L	L	L
W_E	0	L	L	H	L	H	H	H	L	L	L	L	H	H	H	H	L	0	H	L	H	L	L	L	H	H	H	H	L	H	L	L	L	H
v	0	L	H	L	L	L	H	H	H	H	L	H	H	H	L	L	L	0	L	L	H	L	H	H	H	L	H	L	H	H	L	L	L	L
h_i	0	L	L	L	H	H	H	L	H	L	L	H	H	L	H	L	H	0	L	L	L	H	L	H	H	H	L	L	H	H	L	L	H	H
I	0	L	L	H	H	L	L	H	H	L	L	H	L	H	L	H	H	0	L	H	L	L	H	L	H	H	L	L	H	H	H	L	H	H
T_B	0	L	L	H	L	H	H	H	L	H	H	L	L	L	L	L	H	0	L	H	L	H	H	H	L	L	H	H	L	H	L	L	L	H
T_E	0	H	L	L	L	H	L	H	H	L	L	L	H	L	H	L	H	0	L	H	H	L	L	H	L	H	L	H	L	H	L	L	L	L
O_O	0	L	H	L	H	H	L	H	L	H	L	L	L	H	H	L	H	0	L	L	H	H	L	L	H	H	L	L	H	H	L	L	H	H
O_P	0	H	L	H	H	H	L	L	L	H	L	H	H	H	L	L	L	0	H	H	L	H	L	L	L	H	H	L	H	H	L	L	L	L
$P\#$	1	1	1	1	1	1	1	1	1	1	1	1	1	1	1	1	1	2	2	2	2	2	2	2	2	2	2	2	2	2	2	2	2	2

№	45	16	23	24	54	55	63	65	68	2	15	34	37	38	39	43	59	35	10	18	25	36	47	52	60	61	7	9	19	22	27	28	29	51
d_N	0	H	H	H	H	H	H	H	H	L	L	L	L	L	L	L	L	0	H	H	H	H	H	H	H	H	L	L	L	L	L	L	L	L
W_E	0	H	H	L	H	L	L	L	H	H	L	H	L	L	H	L	H	0	L	L	H	H	H	L	H	L	H	L	L	L	H	H	H	L
v	0	L	H	H	H	H	L	L	L	L	L	H	H	L	L	H	H	0	L	H	L	H	H	H	L	L	L	H	L	L	L	H	H	H
h_i	0	L	L	L	H	H	L	H	H	L	H	L	L	L	H	H	H	0	L	L	L	L	H	H	H	H	H	L	H	L	L	H	L	H
I	0	L	L	H	H	L	H	L	H	L	L	L	H	H	L	H	L	0	L	L	H	H	L	H	L	H	L	H	L	H	L	L	H	H
T_B	0	H	H	L	H	L	L	L	H	L	H	L	H	H	L	H	L	0	H	H	L	L	L	H	L	H	H	L	L	H	H	H	L	L
T_E	0	L	H	L	L	H	H	L	H	H	L	H	L	L	L	L	H	0	H	L	L	H	L	H	H	L	L	H	H	L	H	H	L	L
O_O	0	H	L	L	H	H	H	L	L	L	H	L	L	L	H	L	H	0	H	L	H	L	H	H	L	L	L	L	L	H	H	H	L	H
O_P	0	L	H	H	H	H	L	L	L	H	H	L	H	H	L	L	L	0	L	H	L	H	H	H	L	L	H	L	H	H	L	L	L	L
$P\#$	3	3	3	3	3	3	3	3	3	3	3	3	3	3	3	3	3	4	4	4	4	4	4	4	4	4	4	4	4	4	4	4	4	4

With these settings an orthogonal equation system is generated, where the mixing of the main factors only takes place with triple or quadruple interactions. Table II lists the DoE plan, “№” is the experiment number (from 1 to 68), after sorting by the increasing of the mean tensile strength R_m . As visible in Fig. 3, experiment 1 has the minimum R_m while experiment 68 has the maximum R_m .

V. INFLUENCE OF PROCESS PARAMETERS ON R_m AND E

A. General Results from the DoE Plan

With the tensile tests results, the coefficient of determination R^2 is calculated. Its values are 94% for R_m and 93% for E . The measurement series can be assumed successful, and results can be analyzed.

In Fig. 3 all measured tensile strengths R_m and elasticity modulus E are shown, arranged by the mean value of R_m . Thus, six values are marked on each experiment number. These values are the maximum, middle and minimum values of the tensile strength R_m (R_m max, R_m mid and R_m min), as well the maximum, middle and minimum values of the elasticity modulus E (E max, E mid and E min). Due to changes in the process parameters, the R_m values range from 12.9 MPa to 46.6 MPa, and the E values range from 913 MPa to 2930 MPa.

B. Influence of Infill Pattern

Additionally, 24 specimens (4 patterns \times 6 repetitions) were produced and tested with center point values of process parameters: $d_n = 0.4$ mm; $W_E = 1$; $h_l = 0.2$ mm; $I = 70\%$; $O_O = 25\%$; $v = 2000$ mm/min; $T_E = 210$ °C; $T_B = 80$ °C; $O_P = 45$ °. The results are represented in Table III with calculated weight and print time given by the slicer. The triangle infill pattern has the highest strength – its mean value being 30.9 MPa, it is about 3.5 MPa higher than the mean values of the other three

infill patterns. Unlike the pattern’s rectangle and grid, the triangle pattern is printed layer by layer on top of each other, which may explain the higher strength. The least effective is the grid pattern, which has 10.68 % lower R_m , but almost the same weight and print time as triangle pattern. The most economical appears to be the honeycomb pattern, which has the lowest calculated weight and print time.

TABLE III. INFLUENCE OF INFILL PATTERN ON E , R_m , AND SPECIMENS’ WEIGHT (RELATIVE TO TRIANGLE)

Infill pattern	1 Rectangular	2 Grid	3 Triangular	4 Honeycomb
E_{mean} , MPa	1650	1800	2060	1740
$R_{m,mean}$, MPa	27.0	27.5	31.0	27.9
Weight reduction, %	-4.79	-1.63	0.00	-10.40
R_m reduction, %	-11.97	-10.68	0.00	-10.45
Print time reduction, %	-3.33	0.00	0.00	-5.00

The obtained mean values E_{mean} and $R_{m,mean}$ are shown in Fig. 4. They are compared with the mean values $E_{tot mean}$ and $R_{m tot mean}$ obtained from the rest of the tested 216 specimens where the corresponding infill patterns were used. The mean values are close, especially on the R_m chart. This gives grounds for further analyzing the influence of the individual parameters in the set on R_m , based on total mean values.

C. Influence of Nozzle Diameter on Strength

Fig. 5 shows the effect of nozzle diameter in combination of any other parameter in the set on R_m . It is visible that despite of the different nature of the included parameters, the ratio in each of the 16 comparisons is approximately the same and increasing the nozzle diameter leads to higher strength.

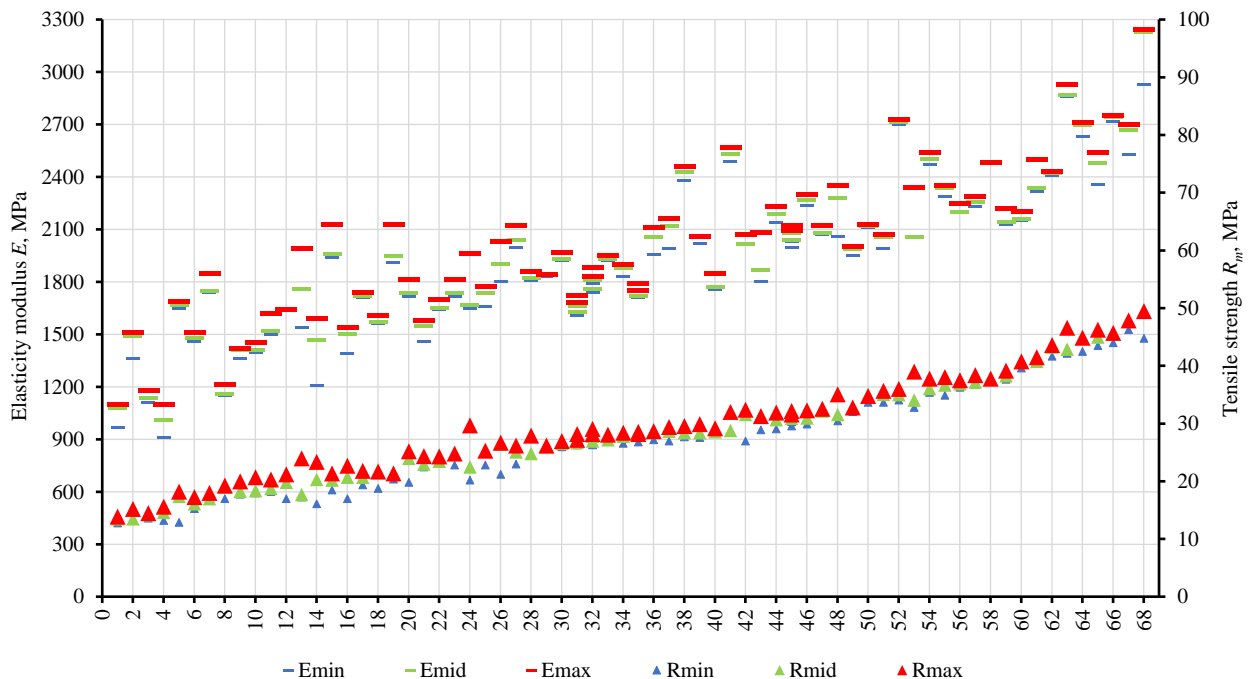


Figure 3. Experimental results for R_m and E of all 216 tensile tests, arranged by the mean value of R_m .

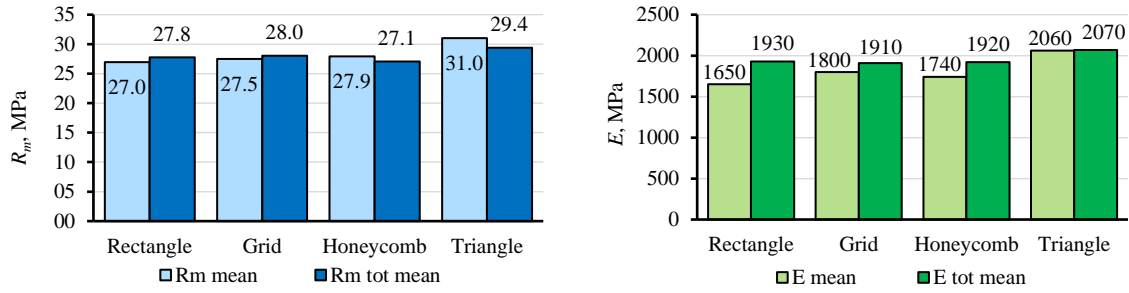


Figure 4. Comparison between the mean values of R_m and E using single parameter difference set (pattern) and multiple parameters difference set.

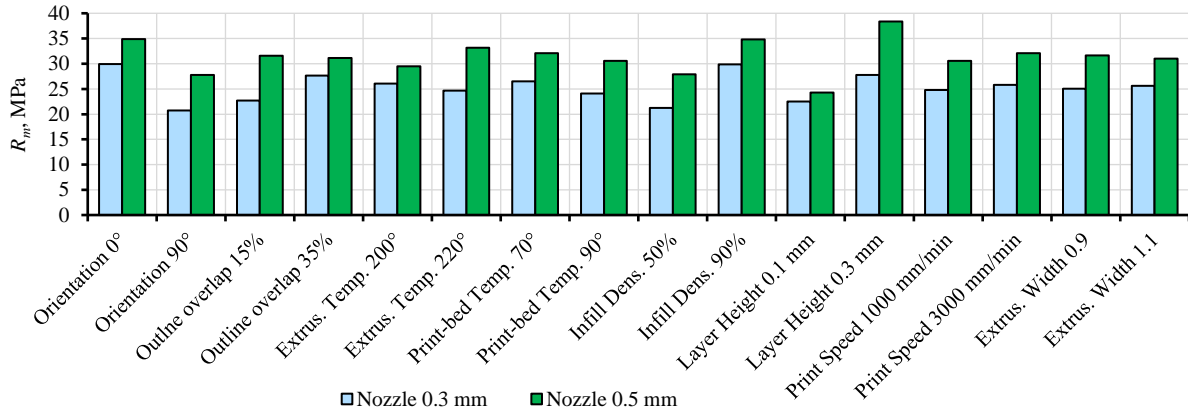


Figure 5. Influence of nozzle diameter in combination with the other parameters in the set and their lower/upper values on R_m .

D. Influence of Single Parameters from DoE on Strength

Fig. 5 gives grounds to further averaging and meaning the results which have a single common value in the set. The result is shown in Fig. 6, which illustrates the influence of each parameter in the set on R_m . The various blue corner points represent the mean strength values of all the experiments where the given value was set. The green center points, represent the mean strength value of measurements mentioned in section B, for comparison. It becomes apparent that changing the nozzle diameter, layer-height, infill percentage, and the print orientation of the top and bottom layers play a dominant role. Of secondary importance is the outline overlap, followed by the temperature of the heat-block and -bed. The speed and extrusion-width-multiplier has virtually no effect on strength.

The larger nozzle diameter and the higher layer thickness ensure that the component approaches the similarity of an injection-molded sample and is therefore more stable. The ratio between the solid shell layers and

the infill layer increases, thus benefiting strength as the cross-sectional area increases. Also, the number of notches is lower and the load is mainly applied to the previously homogeneously melted material. The higher extruder temperature combined with slower printing speed favor bonding of the layers.

The more material is incorporated into the component as infill, the larger the cross-sectional area becomes resulting in lower stresses. To enable the infill to absorb the load it must be connected to the outline shells of the specimen. An increased value for the outline overlap thus favors the strength of the components.

Fig. 7 shows the interaction plot of the main investigated parameters. When an effect of one factor depends on the level of another factor, interaction occurs. This is the case with many process parameters in AM. To visualize the effect, parallel lines in an interaction plot indicate no interaction. The bigger the difference in slope between the lines, the higher is the degree of interaction. It also shows how individual factors contribute to overall mean effect of the parameters seen in Fig. 3.

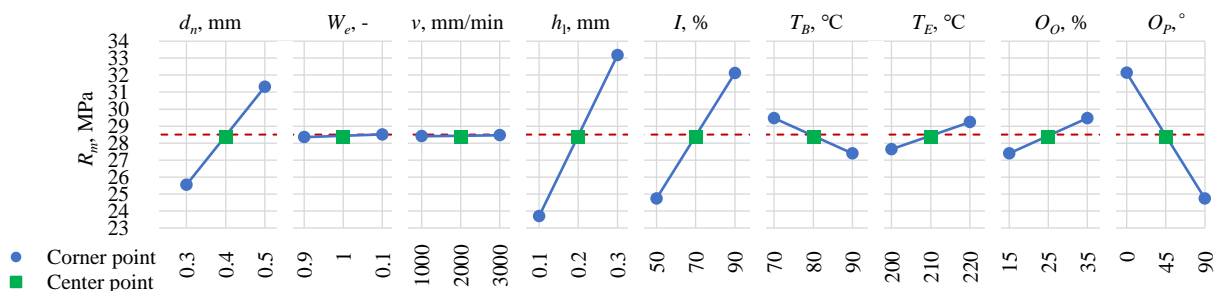


Figure 6. Single parameter influence on R_m .

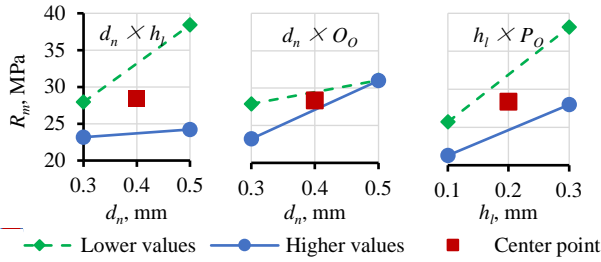


Figure 7. Main interaction plot for tensile strength.

Changing the nozzle diameter d_n creates the biggest effect, also changing the extrusion width. There is a significant interaction between the diameter and layer height. If d_n is decreased without changing the layer-height h_l , the bonding of the strands rapidly decreases [9]. Also, setting the extruder temperature lower and using a smaller nozzle, brings less heat energy per time unit on the already lower existing surface area. Inversely, increasing the h_l with d_n increases the amount of thermal energy. Adding the change in the melt flow for higher temperature as mentioned earlier can explain changes in strength when changing d_n or h_l .

The slicer software issues a warning as soon as the ratio of extrusion-width to height is below 1.2. With a small nozzle diameter and a high layer thickness, the melted filament is not compressed and thus not pushed onto the previously extruded layer. So the strength between the layers decreases considerably. Also, the contact area to the previous layer is reduced. This ratio is undercut with the combination of 0.3 mm nozzle diameter and 0.3 mm layer height, resulting in poorer stress. Hence the warning by the slicer software is justified and cannot be compensated by other parameters. Changes in extrusion-multiplier values are not recommended.

Changes in the top and bottom layer orientation results in stressing different interfaces within the cross-section of the specimen while testing. An orientation of 90° results in specimens where upper and lower layers experience stress concentrations between the strands, resulting in poorer strength. This effect can partly be compensated by increasing the outline overlap as seen from the interaction plot. Since the normal stress depends on the cross-sectional area, it is expected that changes in the infill percentage effect strength, since the cross-sectional area is being heavily manipulated.

E. Influence of Additional Parameters on Strength

The effects of filament color and the time between the specimens production as well as the tensile test (time-to-test) may be significant and should be estimated [11]. The results of testing three specimens on each filament color (black or white) and six specimens on each time-to-test (1 day or 30 days) are shown in Fig. 8. Time-to-test and thus the possible influence of water absorption between print and tensile test do not play a significant role in the measurement series. Furthermore, changing the filament color from black to white has very little influence on the tensile strength.

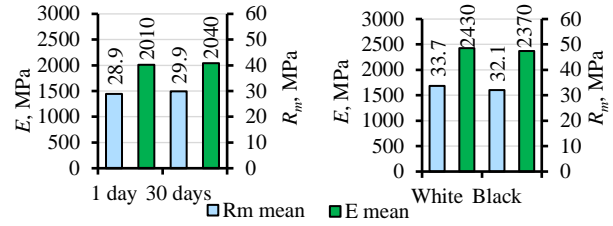


Figure 8. Influences of filament color and time-to-test on R_m and E .

VI. OPTIMIZATION

Using the data from the DoE and a linear regression considering interaction effects [12], created by the statistical software (1) is proposed for prediction of R_m :

$$R_m = 34.926 - 192.2 D_N + 140.3 W_E + 0.00852 v - 45.3 h_l - 0.730 I + 0.242 T_B - 0.256 T_E - 1.894 O_O + 0.1406 O_P - 32.300 d_N W + 0.00708 d_N v + 235.800 d_N h_l - 0.1376 d_N I + 0.242 d_N T_B + 1.01100 d_N T_E - 1.2980 d_N O_O + 0.0516 d_N O_P - 0.00766 W_E V - 47.000 W_E h_l - 0.1704 W_E I - 0.13400 W_E T_B - 0.4420 W_E T_E + 0.797 W_E O_O - 0.14170 W_E O_P - 0.007240 v h_l - 0.000018 v I + 0.00001 V T_B - 0.000005 v T_E - 0.000051 v O_O + 0.000013 v O_P - 0.500600 h_l I - 0.017 h_l T_B + 0.45800 h_l T_E + 0.001603 I T_B + 0.005124 I T_E + 0.00466 I O_O - 0.000993 I O_P - 0.00249 T_B T_E + 0.00296 T_B O_O + 0.000256 T_B O_P + 0.00600 T_E O_O - 0.000378 T_E O_P. \tag{1}$$

Using the response optimizing feature of the statistics software, equation (1) was solved for finding the optimum parameters set for the investigated steps shown in Table I. Quadratic terms are not considered since their influence is negligible and the predicted values match the experimental data. Table IV shows the returned set.

TABLE IV. OPTIMUM PARAMETERS SET

d_n , mm	W_E	h_l , mm	I , %	O_O , %	v , mm/min	T_E , °C	T_B , °C	O_P , °	$P\#$
0.5	1.1	0.3	90	35	1000	220	70	0	3

The model predicts a tensile strength of 52.93 ± 2.26 MPa with 95% confidence interval. This means that there is a 95% chance that the mean tensile strength of specimens printed with optimized parameter-sets will be between 50.67 MPa and 55.19 MPa. To validate this, three tensile specimens were printed with these settings and tested in tension. The results are shown and compared in Table V. These optimized specimens have a mean strength of 51.2 MPa and are thus 6.9% stronger than the mean tensile strength of the strongest specimens from the DoE ($\Delta R_{m, mean}$ in Table V). This shows that equation (1) can be successfully used to predict R_m .

TABLE V. RESULTS OF OPTIMIZATION.

Result	$R_{m, min}$, MPa	$R_{m, mid}$, MPa	$R_{m, max}$, MPa	$R_{m, mean}$, MPa	$\Delta R_{m, mean}$, %
Best of DoE	44.8	49.4	49.5	47.9	-
Optimum parameters set	49.9	51.2	52.4	51.2	6.9%
Prediction with 95% CI	50.67	52.93	55.19	52.93	10.5%

VII. CONCLUSION

As a result of testing 216 specimens, produced with variation of 10 parameters using the DoE approach, we receive tensile strength ranged from 12.8 MPa to 49.5 MPa. Based on this experimental data and using statistical model with linear regression, we obtained an optimal parameter set. Using this set, we produced optimized specimens which achieved a mean tensile strength almost 7% higher than the best of DoE.

Significant influences, like the nozzle diameter, top and bottom layer orientation, infill amount and layer height, were shown. Due to the interactions caused by the resolution of the design plan, the influence of all parameters could not be measured individually. Furthermore, age of up 30 days and the filament color have very little influence on strength.

With the created statistical model, we proposed an equation for prediction of tensile strength. The equation results were verified. The difference between the predicted and experimentally received value of R_m is negligibly small. Research suggests further studying the effects of higher printing speeds, thus improving efficiency, as no significant influence was observed using the values in the experiments. It would be relevant to study how the model may be applicable to stronger filament materials.

CONFLICT OF INTEREST

The authors declare no conflict of interest.

AUTHOR CONTRIBUTIONS

Maurice Schwicker together with students of the University of Applied Sciences Kaiserslautern, developed and commissioned the test stand and conducted the experiments. Nikolay Nikolov, Maurice Schwicker and Marco Häfel and analyzed the data and wrote the paper; all authors had approved the final version.

ACKNOWLEDGMENT

The authors would like to thank the “Research-Fond Rhineland-Palatinate”, “BMBF Project research learning”, and Research and Development Sector at Technical University of Sofia for providing valuable financial support.

REFERENCES

- [1] C. Dai, C. C. L. Wang, C. Wu, S. Lefebvre, G. Fang, and Y. J. Liu, “Support-free volume printing by multi-axis motion,” *ACM Trans. Graph.*, vol. 37, no. 4, p. 13, 2018.
- [2] H. C. Song, N. Ray, D. Sokolov, and S. Lefebvre, “Anti-aliasing for fused filament deposition,” *Comput. Des.*, vol. 89, pp. 25–34, 2017.
- [3] R. J. A. Allen and R. S. Trask, “An experimental demonstration of effective curved layer fused filament fabrication utilising a parallel deposition robot,” *Addit. Manuf.*, vol. 8, pp. 78–87, 2015.
- [4] S. Riecker, O. Andersen, S. Hein, T. Studnitzky, and B. Kieback, *Integrated Process Line for Fused Filament Fabrication of Metallic Parts Using Metal Powder Loaded Filaments*, 2017.
- [5] S. Ahn, M. Montero, D. Odell, S. Roundy, and P. K. Wright, “Anisotropic material properties of fused deposition modeling ABS,” *Rapid Prototyp. J.*, vol. 8, no. 4, pp. 248–257, Jan. 2002.
- [6] C. Y. Lee and C. Y. Liu, “The influence of forced-air cooling on a 3D printed PLA part manufactured by fused filament fabrication,” *Addit. Manuf.*, vol. 25, pp. 196–203, 2019.
- [7] N. G. Tanikella, B. Wittbrodt, and J. M. Pearce, “Tensile strength of commercial polymer materials for fused filament fabrication 3D printing,” *Addit. Manuf.*, vol. 15, pp. 40–47, 2017.
- [8] F. Knoop, A. Kloke, and V. Schoeppner, “Quality improvement of FDM parts by parameter optimization,” in *Proc. AIP Conference Proceedings*, 2017, vol. 1914, no. 1, p. 190001.
- [9] V. E. Kuznetsov, A. N. Solonin, O. D. Urzhumtsev, R. Schilling, and A. G. Tavitov, “Strength of PLA components fabricated with fused deposition technology using a desktop 3D printer as a function of geometrical parameters of the process,” *Polymers (Basel)*, vol. 10, no. 3, p. 313, 2018.
- [10] *Plastics - Determination of tensile properties - Part 2: Test Conditions for Moulding and Extrusion Plastics*, ISO Standard 527-2, 2012.
- [11] B. Wittbrodt and J. M. Pearce, “The effects of PLA color on material properties of 3-D printed components,” *Addit. Manuf.*, vol. 8, pp. 110–116, 2015.
- [12] G. James, D. Witten, T. Hastie, and R. Tibshirani, “Linear Regression,” in *An Introduction to Statistical Learning*, Los Angeles, USA: Springer, 2013, pp. 59–120.

Copyright © 2022 by the authors. This is an open access article distributed under the Creative Commons Attribution License (CC BY-NC-ND 4.0), which permits use, distribution and reproduction in any medium, provided that the article is properly cited, the use is non-commercial and no modifications or adaptations are made.

Maurice Schwicker was born in Wiesbaden, Germany. He has Diploma (FH) and M. Eng. degrees in mechanical engineering from the University of Applied Sciences RheinMain and Kaiserslautern. He is currently a research fellow at the University of Applied Sciences Kaiserslautern, Department of Applied Engineering Sciences. His research interests include Additive Manufacturing with a focus on Fused Deposition Modeling using Robotics and Selective Laser Sintering of polymers.

Nikolay Nikolov was born in Sofia, Bulgaria. He has B.S., M.S, and Ph.D. degrees in mechanical engineering from Technical University of Sofia. He is currently associated professor in Technical University of Sofia, Department of Mechanics. His research interests include Strength of Materials, strength-related numerical modeling, strength- and deformational analysis of details and structures. His current research projects include influence of additive manufacturing process parameters on strength, and influence of corrosion on strength.

Marco Häfel was born in Kaiserslautern, Germany. He has M. Eng degree in mechanical engineering from the University of Applied Sciences Kaiserslautern. He is currently a research fellow at the University of Applied Sciences Kaiserslautern, Department of Applied Engineering Sciences. His research interests include Optical Metrology and Additive Manufacturing with Focus on Fused Deposition Modelling.